

## Electrochemical Behavior of Electrodeposited Ni-P Coatings in Acidic Solutions

O.V. Dolgikh,\* N.V. Sotskaya, L.V. Sapronova

Voronezh State University, 1, Universitetskaya Sq., 394006 Voronezh, Russia

(Received 15 June 2012; published online 21 August 2012)

The paper is devoted to the investigation of cathodic and anodic behavior of electrodeposited Ni-P alloys of different composition in H<sub>2</sub>SO<sub>4</sub> solutions. It was established that increase of phosphorous content enhances anticorrosion ability of Ni-P coatings and decreases their catalytic activity toward to hydrogen evolution reaction. The most probable mechanism of this reaction was suggested on the basis of analysis of experimental data. It assumes that at low overpotentials hydrogen evolution proceeds by Volmer-Heyrovsky route with limiting step of charge transfer. At higher potentials Volmer-Tafel mechanism with slow chemical recombination step takes place.

**Keywords:** Ni-P Coatings, Anticorrosion Ability, Catalytic Activity, Hydrogen Evolution Reaction, Mechanism.

PACS numbers: 81.40.Np

### 1. INTRODUCTION

Electrodeposited Ni-P alloys are widely used in industry both as corrosion protective and catalytically active materials. It is generally accepted that Ni-P coatings exhibit higher corrosion resistance than pure nickel in acidic and neutral media, which is attributed to the suppression of their anodic dissolution [1-4]. At the same time conflicting reports were published in what concerns their catalytic activity to hydrogen evolution reaction (HER). It follows from published results that some Ni-P electrodes are considerably active [5-7], while other electrodes even with comparable phosphorous content are significantly less active [8, 9]. The reason of such uncertainties might be the differences of electrolytes compositions, deposition regimes, coatings thickness, etc. So, the aim of this work is to obtain Ni-P coatings in the wide range of P content and to investigate their corrosion resistance and catalytic activity to HER in 0.05 M H<sub>2</sub>SO<sub>4</sub> solutions.

### 2. EXPERIMENTAL

Prior to the experiments, the working nickel electrode ( $S_{\text{met.Ni}} = 0.22 \text{ cm}^2$ ) was abraded with emery paper; each successive paper was finer grained. Then, it was polished with magnesium oxide and soft chamois and degreased with ethyl alcohol. After every operation, the electrode was thoroughly washed with distilled water. The Ni-P coatings of various compositions were deposited from the electrolyte containing 0.08 M NiCl<sub>2</sub>, 0.20 M NH<sub>2</sub>CH<sub>2</sub>COOH, 0.12 M CH<sub>3</sub>COONa, and (0–1.00) M NaH<sub>2</sub>PO<sub>2</sub> (all compounds were of reagent grade). The coatings were deposited under galvanostatic conditions ( $i = -5 \text{ mA/cm}^2$ ,  $\tau = 1000 \text{ s}$ ). Average deposit thickness was  $1.19 \pm 0.14 \text{ }\mu\text{m}$ .

Electrochemical behavior of Ni-P coatings was studied in 0.05 M H<sub>2</sub>SO<sub>4</sub> deaerated solution. Quasi-steady state polarization curves were measured from open-circuit potential at first in cathodic and then in anodic direction with scan rate  $v = 1 \text{ mV/s}$ . Potential-relaxation transients were recorded after interruption

of prior galvanostatic polarization ( $\tau = 400 \text{ s}$ ). Polarization currents were chosen individually for each alloy.

Experiments were performed in a conventional three-electrode cell. A copper-sulfate electrode ( $E = -0.335 \text{ V}$ ) was used as the reference electrode; a platinum electrode with large surface area was used as the auxiliary electrode. The polarization was imposed with an IPC-compact potentiostat. In the paper, all potentials are given with respect to the s.h.e.

### 3. RESULTS AND DISCUSSION

The electrolytes used for coatings electrodeposition allow us to produce Ni-P alloys with phosphorous content from 0.1 to 12.6 wt. %. Structure and morphology of obtained coatings were thoroughly described in our previous work [10]. Coatings with P content less than 7 wt. % were crystalline, while others were X-ray amorphous and consisted of nanocrystalline nickel and its phosphides. Let us consider the effect of Ni-P composition on the main characteristics of their electrochemical behavior.

#### 3.1 Corrosion potential and rates of anodic and cathodic reactions

Quasi-steady state polarization curves obtained in 0.05 M H<sub>2</sub>SO<sub>4</sub> solution on studied Ni-P alloys are selectively shown in Fig. 1. Main characteristics of Ni-P electrochemical behavior such as corrosion potentials ( $E_{\text{cor}}$ ) and rates of cathodic ( $i_c$ ) and anodic ( $i_a$ ) reactions were defined from polarization curves. The reaction rates were estimated by current densities measured at  $E_c = -0.40 \text{ V}$  and  $E_a = +0.15 \text{ V}$  respectively. All these parameters are summarized in Table 1.

Corrosion potential becomes more positive with increase of phosphorous content in electrodeposited Ni-P coatings (see Table 1), indicating the improvement of their anticorrosion properties. Furthermore, rate of anodic reaction for phosphorous-rich Ni-P alloys three times lower than for pure nickel. This result also supports that the increase in phosphorous content enhances the anticorrosion ability of Ni-P coatings in acidic media.

\* [dov@chem.vsu.ru](mailto:dov@chem.vsu.ru)

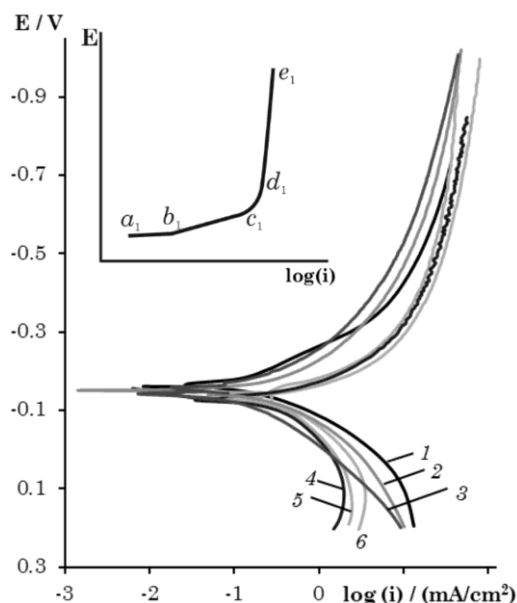


**Fig. 1** – E-log(i) polarization curves measured in 0.05 M  $H_2SO_4$  solution on electrodeposited Ni-P coatings with P content: 1 – 0; 2 – 0.5; 3 – 1.4; 4 – 3.0; 5 – 6.5; 6 – 12.1 wt. %. **Inset:** selection of linear plots on the cathodic polarization curves

In the contrast to the anodic process, the rate of cathodic reaction slightly decreases with rise of P content up to 6.5 wt. % and then the process is substantially accelerated.

According to the general view, the rate of hydrogen evolution reaction is defined, on the one hand, by the catalytic properties of the material, which depend on their electronic structure, and, on the other hand, by its real surface area, which is associated with roughness and porosity of the coatings. In order to eliminate the contribution of surface development in the rate of cathodic reaction we normalized cathodic current densities  $i_c$  to the corresponding relative roughness factor values  $f_r = S_{Ni-P} / S_{met.Ni}$ , which were determined for Ni-P coatings of different composition earlier by potential-relaxation transients method (the values of  $f_r$  were found to change from 0.75 for pure Ni-coating to 34.5 for Ni-12.6P) [10]. The same normalization procedure was done for anodic current densities. The results are presented in Table 1. It can be seen that both anodic and cathodic reactions decelerate with increase of phosphorous content. Observed acceleration of HER by Ni-P coatings with P content higher than 6.5 wt. % is the result of substantial surface development only.

**Table 1** – Corrosion potentials  $E_{cor}$  and rates of cathodic ( $i_c$ ) and anodic ( $i_a$ ) reactions ( $f_r$  – relative roughness factor).

[P], wt. %	$E_{cor}$ , V	log (i) (mA/cm <sup>2</sup> )		log (i / $f_r$ ) (mA/cm <sup>2</sup> )	
		cathodic	anodic	cathodic	anodic
0.0	-0.160	+0.820	+0.945	+0.945	+1.070
0.5	-0.151	+0.825	+0.900	+0.939	+1.040
1.4	-0.148	+0.659	+0.799	+0.772	+0.591
3.0	-0.122	+1.207	+0.279	+0.974	+0.046
6.5	-0.129	+1.303	+0.535	+0.304	-0.460
10.1	-0.137	+1.209	+0.468	-0.380	-1.120
12.6	-0.127	+1.171	+0.391	-0.365	-1.145

### 3.2 Mechanism of hydrogen evolution reaction

Despite the number of investigations devoted to the hydrogen evolution on Ni-P alloys, mechanism of the process still remains uncertain. In order to establish the mechanism of HER it is necessary to obtain and analyze some diagnostic criteria, namely Tafel slopes of polarization curves, reaction order in hydrogen ions, slopes of  $E - \log(dE/d\tau)$  dependencies, sign of  $dC_{tot}/dE$  derivative [11-13].

As it can be seen from Fig. 1, cathodic polarization curves in  $E - \log(i)$  coordinates are rather nonlinear. So, we selected two linear plots at low and high overpotentials (see inset in Fig. 1). Plot  $b_1c_1$  with Tafel slope  $b = 0.08-0.15$  V can be found only in voltammograms for Ni-P alloys with phosphorous content up to ~6.5 wt. %. Plot  $d_1e_1$  with higher Tafel slopes (0.37-0.75 V) is typical for all investigated alloys. Both Tafel slopes increase with phosphorous content in Ni-P coatings. Some additional information can be obtained from reaction order in hydrogen ions. Its values virtually don't depend on potential and are close to unity regardless of P content in Ni-P alloy.

Tafel slopes  $b_c$  and reaction order values  $R_H$  are listed in Table 2.

**Table 2** – Tafel slopes  $b_c$  and reaction orders in hydrogen ions  $R_H$  for Ni-P alloys of different composition

[P], wt. %	$b_k = dE/d\log(i)$		$R_H = d\log(i)/dpH$
	plot $b_1c_1$	plot $d_1e_1$	
Ni <sub>met.</sub>	0.133	–	0.91±0.09
0.0	0.084	0.371	0.64±0.02
0.2	0.090	0.417	0.87±0.05
1.3	0.107	0.423	1.03±0.11
3.0	0.107	0.465	0.87±0.07
6.3	0.150	0.412	0.89±0.03
8.2	–	0.659	0.85±0.05
11.9	–	0.607	0.88±0.02
12.6	–	0.594	0.86±0.04

Potential-relaxation transients were recorded for metallic nickel electrode and some Ni-P alloys. They are shown in Fig. 2. Slope of these dependencies in  $E - \log(dE/d\tau)$  coordinates is also diagnostic criterion for elucidation of HER mechanism [14]:

$$E(\tau) = b' \lg\left(\frac{dE}{d\tau}\right) + b' \lg(C_H) - b' \lg(i_0)$$

As in the case of polarization curves,  $E - \log(dE/d\tau)$  plots are nonlinear, therefore we selected two linear regions:  $b_2c_2$  at low cathodic overpotentials, and  $d_2e_2$  at high overpotentials (see inset in Fig. 2). Slopes of these plots are listed in Table 3. Their values correspond to tafel slopes for polarization curves.

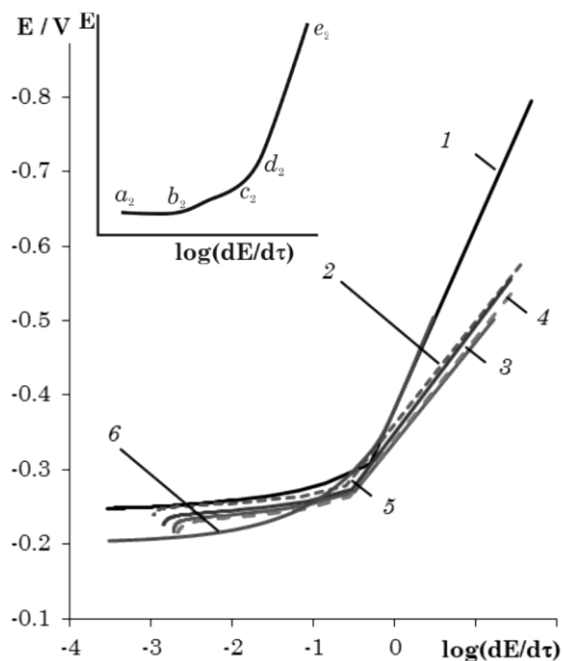


**Fig. 2** –  $E - \log(dE/d\tau)$  plots obtained from potential-relaxation transients measured on metallic Ni (1) and electrodeposited Ni-P coatings with P content: 2 – 0; 3 – 3.0; 4 – 6.5; 5 – 8.8; 6 – 12.6 wt.%. Inset: selection of linear sections

Important information about HER mechanism can be obtained from dependencies of interfacial capacitance on potential. Total interfacial capacitance  $C_{tot} = C_H + C_{dl}$  was calculated by combined processing of respective polarization curves and potential-relaxation transients. Derived dependencies of  $C_{tot}$  on potential for metallic nickel and some Ni-P coatings are shown in Fig. 3. They are characterized by relatively high (about  $100 \mu\text{F}/\text{cm}^2$ ) values of interfacial capacitance in the vicinity of equilibrium potential and sharp decrease with rise of cathodic potential.

**Table 3** – Slopes of  $E - \log(dE/d\tau)$  dependencies for Ni-P alloys of different composition

[P], wt.%	$dE/d\log(dE/d\tau)$	
	plot $b_2c_2$	plot $d_2e_2$
Ni <sub>met.</sub>	0.010	0.213
0.0	0.011	0.138
3.0	0.020	0.133
6.3	0.021	0.137
8.2	0.005	0.144
12.6	0.011	0.161

Unambiguous establishment of HER mechanism on electrodeposited Ni-P alloys is a problem, which cannot be solved on the basis of analysis of one criterion only. Even when we use the set of diagnostic criteria, some uncertainty of reaction stages nature remains because

of the deviation of experimentally obtained parameters from theoretical ones due to participation of adsorbed intermediates in charge transfer step. Therefore, we can only talk about the most probable route of the process under study.

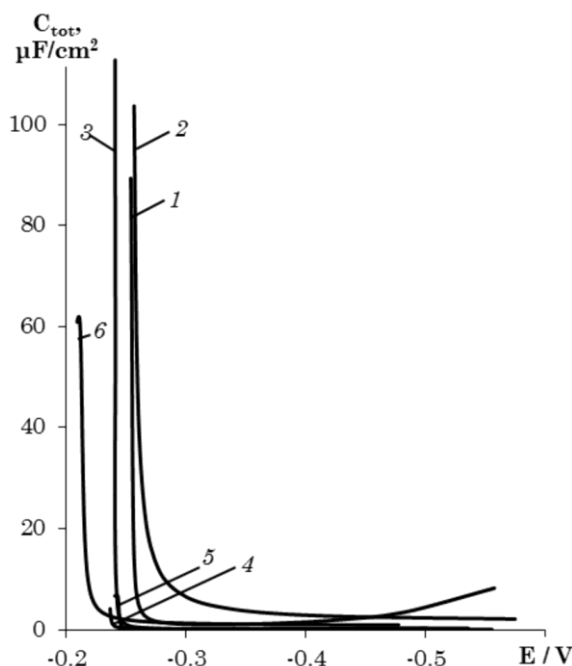


**Fig. 3** – Dependencies of interfacial capacitance  $C_{tot}$  on potential for metallic Ni (1) and electrodeposited Ni-P coatings with P content: 2 – 0; 3 – 3.0; 4 – 6.5; 5 – 8.8; 6 – 12.6 wt.%

The analysis was carried out separately for regions of low and high overpotentials. It was found that hydrogen evolution reaction on electrodeposited Ni-P alloys obeys general laws, regardless of the phosphorous content. At low overpotentials it proceeds by Volmer-Heyrovsky route with limiting stage of charge transfer. This is evidenced, mainly, by dependency of interfacial capacitance on potential ( $dC_{tot}/dE > 0$ ) [12]. At high cathodic potentials Volmer-Tafel mechanism takes place with slow step of chemical recombination, which is testified by very high slopes of linear plots  $d_1e_1$  and  $d_2e_2$  on voltammograms and potential-relaxation transients respectively [12, 13].

The influence of alloy composition appears in variation of tafel slopes both at low and high overpotentials, probably due to changes in charge transfer coefficients of Volmer stage  $\alpha_1$  and surface coverage by adsorbed hydrogen  $\theta_H$  [11]. At low cathodic potentials main contribution to the change of tafel slope gives the reduction of  $\alpha_1$  with increase of phosphorous content up to 6.5 wt. %. At high overpotentials variation of surface coverage plays a major role in increase of tafel slope.

## REFERENCES

1. R.B. Diegle, N.R. Sorensen, C.R. Clayton, M.A. Helfand, Y.C. Yu, *J. Electrochem. Soc.* **135**, 1085 (1988)
2. J. Hajdu, *Plat. Surf. Finish.* **83**, 29 (1996).
3. P. Peeters, G.v.d. Hoorn, T. Daenen, A. Kurowski, G. Staikov, *Electrochim. Acta* **47**, 161 (2001).
4. A. Krolikowski, B. Karbownicka, O. Jaklewicz, *Electrochim. Acta.* **51**, 6120 (2006).
5. I. Paseka, J. Velicka, *Electrochim. Acta* **42**, 237 (1997).
6. R.K. Sheverdami, A. Lasia, *J. Electrochem. Soc.* **144**, 511 (1997).
7. T. Burchardt, *Int. J. Hydrogen Energ.* **25**, 627 (2000).
8. J.J. Podesta, R.C.V. Piatti, A.J. Arvia, P. Ekundge, K. Juttner, G. Kreysa, *Int. Hydrogen Energ.* **17**, 9 (1992).
9. A. Krolikowski, A. Wiecko, *Electrochim. Acta* **47**, 2065 (2002).
10. O.V. Dolgikh, N.V. Sotskaya, Yu.G. Kravtsova, *Russ. J. Electrochem.* **46**, 918 (2010).
11. B.V. Tilak, C.-P. Chen, *J. Appl. Electrochem.* **23**, 631 (1993).
12. V.V. Kuznetsov, G. Khaldeev V.I. Kichigin, *Navodornance of metals in solutions of electrolytes* (Mashinostroenie: 1993) (in Russian).
13. A.V. Vvedensky, I.A. Gutorov, N.B. Morozov, *Cond. Environment and Interface Grains* **12**, 288 (2010) (in Russian).
14. B.E. Conway, L. Bai, D.F. Tessier, *J. Electroanal. Chem.* **161**, 39 (1984).